Standard Solar Model

Kevin France

Department of Physics and Astronomy, Johns Hopkins University, Baltimore, MD 21218

ABSTRACT

The standard solar model is one of the most complete and successful theories in modern astronomy. I discuss the basic assumptions of the model: hydrostatic equilibrium, energy transport, thermonuclear reactions, and initial conditions. The successes and failures of the model are illustrated, followed by a brief analysis of the model data. A discussion of what can be learned from the model data is presented using composition, energy production, and convection as examples.

Subject headings: models: solar—thermonuclear energy: production, transport

1. Basic Assumptions

The Sun is the most prominent object in our sky, and understanding it has been one of the primary focuses since the birth of modern astronomy. Additionally, after the realization that the Sun was itself a star, solar research became a means for investigating conditions too distant to observe directly. Starting in the early twentieth century, astronomers began building a model of the Sun that would accurately predict the Sun's observable features. If the model can accurately predict what is observed, then it is reasonable to assume that it can accurately tell astronomers about what they cannot observe, both inside the Sun and its behavior at other epochs. This model is known as the standard solar model, and it has been in a state of constant evolution since its inception.

The standard solar model has four basic assumptions, the first being that the sun evolves in hydrostatic equilibrium (3). Hydrostatic equilibrium implies a local balance between pressure and gravity, can be expressed as:

$$\frac{dP}{dr} = -\frac{Gm\rho}{r^2} \tag{1}$$

where P is the pressure, ρ is the density, and m is the mass contained inside the radius r. To describe this condition in detail, one must specify the temperature, density, and composition of the stellar material. This combination is known as an equation of state, the simplest of which being the ideal gas law:

$$P = \frac{\rho T \mathcal{R}}{\mu} \tag{2}$$

where μ is the mean molecular weight, T is the temperature of the material, and $\mathcal{R}$ is a constant (4).

The second assumption of the standard solar model is that energy can be transferred in the star via radiation, conduction, convection, and neutrino losses (3; 4). Radiation and convection are the dominant forms of energy transport, and a measure of energy flow is the temperature gradient produced through each process:

$$\frac{dT}{dr} = -\frac{3\kappa\rho L}{16\pi acr^2T^3} \tag{3}$$

and

$$\frac{dT}{dr} = \left(1-\frac{1}{\gamma}\right)\left(\frac{T}{P}\right)\frac{dP}{dr} \tag{4}$$

for radiative and conductive transport, respectively, where κ is the opacity of the stellar material, L is the luminosity, and γ is the ratio of specific heats, C_P/C_V. These two processes vary in their efficiencies depending on the local values at a given point inside the star.

The third assumption of the model is that thermonuclear reactions are the only source of energy production inside the star (3). The thermonuclear reactions that take place in the core of a star like our Sun are processes that fuse hydrogen nuclei into helium nuclei, releasing copious quantities of energy in the process. There are two processes, or chains of reactions, that are responsible for the fusion in our Sun, these are the proton-proton (pp) chain and the carbon-nitrogen-oxygen (CNO) chain. These chains are described in more detail below. Fusion reactions require high densities and temperatures to take place, and therefore are predominantly found in stellar cores. A measure of the luminosity in star created by these reactions is given by:

$$\frac{dL}{dr} = 4\pi r^2\rho\varepsilon \tag{5}$$

where ε is the energy production rate [ergs g^{-1} s^{-1}] (6).

The final assumption of the standard solar model is that the sun was initially of a homogeneous, primordial composition, and highly convective at its main sequence turn on. Since heavy elements are neither created nor destroyed in the thermonuclear reactions in a solar-type star, they provide a record of the initial abundances, and only the relative amounts of hydrogen and ^{4}helium are an indicator of stellar evolution. The standard solar model has been successful over its lifetime in reproducing the conditions observed today and producing scenarios for stellar interiors that are in agreement with standard physics and subsequent measurements. For example, Turck-Chieze *et al*. (5) (5) define their model successful if it converges to solar values with errors less than given in the table below.

Quantity	**Acceptable Error**
Solar Luminosity, $L_\odot$	$\pm\ 5 \times 10^{-3}\ L_\odot$
Solar Age, $t_\odot$	$\pm\ 0.1 \times 10^9$ yr
Solar Radius, $R_\odot$	$\pm\ 5 \times 10^{-4}\ R_\odot$

Until very recently, the biggest shortcoming of the standard solar model was the solar neutrino prediction. Experiments on the earth set an upper bound for the number of neutrinos that could be produced in the sun, and these numbers fell well short of the number of neutrinos predicted by the standard model. Solving this problem was the focus of solar model research over the last 30 years. The answer was recently found by (2) when they measured oscillations in the type of neutrinos emitted from the sun.

2. Standard Solar Model Data

The next step is to insert the model assumptions into a code that will generate values for mass, luminosity, pressure, density, and composition for each value of stellar radius. These essential physical quantities can be combined in various ways to shed light on the processes occurring to create the physical conditions inside the star.

2.1. Composition

Equation (2) can be inverted to solve for the mean molecular weight for a given region, which allows one to observe the overall change in composition throughout the star. This figure shows the decline in molecular weight with increasing radius. This decline is a product of the thermonuclear reactions that are powering the star. As mentioned above, during stellar evolution, hydrogen is converted into helium in the hot, dense core. That the star is no longer of a homogeneous composition is a clear indication of its evolution. The ^{4}helium content in the core of the star is enhanced as the star uses up its fuel, which can be seen from the nuclear chains mentioned above. The dominant process for converting hydrogen to helium in a solar-type star is the *pp* chain, where:

$$\begin{gathered} p+p \rightarrow D+e^{+}+\nu_e \\ D+p \rightarrow ^3He+\gamma \\ ^3He+^3He \rightarrow ^4He+p+p \end{gathered} \tag{6}$$

is known as *pp*-I, and is responsible for 84.6 % of solar energy generation, where p are protons, D are deuterium nuclei, and ν and γ are emitted neutrinos and photons, respectively. The star has another option, *pp*-II, which occurs if:

$$^3He+^4He \rightarrow ^7Be+\gamma \tag{7}$$

followed by further steps leading to the creation of ^{4}helium. This process produces 13.8 % of solar energy.

The other process mentioned above is the *CNO* chain, which also converts hydrogen into ^{4}helium, but uses carbon, nitrogen, and oxygen nuclei as catalysts. This process does not dominate until 20-25 million degrees Kelvin, so in our Sun, where the core temperature is $>$ 16 million Kelvin, this process is only secondary, producing the remaining 1.6 % of solar energy. The *CNO* chain plays another important role in the core of a star, which is to change its composition. Carbon is converted into nitrogen through the *CNO* process, which should be observed as an enhancement of nitrogen and a depletion of carbon in the core. Both carbon and nitrogen go through the catalytic cycle about a dozen times over the life of the Sun, whereas oxygen nuclei only go through a fraction of a cycle (1). Figure 2 illustrates the fraction of stellar material composed of hydrogen and ^{4}helium as a function of radius as well as the *CNO* catalysts compared to ^{4}helium.

2.2. Energy Production Regions

As discussed above, the thermonuclear reactions that power the sun require the high temperatures and densities associated with the core of the Sun. Equation (5) can be rewritten to solve for the energy production rate. The energy production rate is seen to fall off appreciably by 0.2 $R_\odot$. This fact is further seen by noticing that the Sun's luminosity has reached its full value by 0.2 $R_\odot$, telling us that all of the energy production took place inside that radius. Similarly, Bahcall *et al*. (1) find 95 % of solar luminosity produced within 0.21 $R_\odot$, and a similar calculation of energy production finds its peak at 0.09 $R_\odot$ with half-maximum at 0.16 $R_\odot$. Another interesting question is to ask how different is the Sun today than at its main sequence turn on. This can be answered by taking a successful model and comparing its initial conditions with present values. Turck-Chieze *et al*. (5) find that since main sequence turn on, the Sun's luminosity has increased by 30 %, the radius has increased by 15 %, the core temperature has increased by 8 %, the core pressure has increased by 61 %, and the central hydrogen abundance has been depleted by 50 %.

2.3. Convection

In the outer regions of a star, local perturbations may cause discrete regions to become unstable. The region becomes unstable when its density becomes appreciably different than its surroundings. This density change will result in a buoyancy force acting on the region and causing it to rise or fall. This bulk motion of material is convection, and is an important process that influences stellar structure by carrying energy and mixing stellar material (4). If we assume that the region changes adiabatically, and that the surrounding region is predominantly transporting energy via radiation, we can write down a condition for the region to be stable:

$$\nabla_{rad} < \nabla_{adb} \tag{8}$$

which is known as the *Schwarzchild stability criterion.* The ∇s are temperature gradients, and are defined as:

$$\nabla_{rad} = \frac{3\kappa LP}{16\pi acGmT^4} \tag{9}$$

the radiative temperature gradient, and:

$$\nabla_{adb} = \nabla_{region} = \left(\frac{d\ln T}{d\ln P}\right)_{region} \tag{10}$$

the adiabatic temperature gradient (4). When the stability criterion is violated (ie-when the radiative temperature gradient is greater than the adiabatic temperature gradient), the region will become unstable and convection will begin. When convection is most efficient, the adiabatic temperature gradient is roughly equal to the total gradient (ie- $\nabla_{adb} \approx \nabla_{tot}$) (4). These gradients can be calculated and one can determine where convection will play a significant role in the stellar structure. Figure 4 shows that in the outer regions of the star, the radiative transport is insufficient for carrying all of the energy. Convection is seen to be transporting its maximum fraction of stellar energy near 0.7 $R_\odot$ (6).

3. Closing

Appendix A contains a set of figures that can be produced with the data from the standard solar model. They are mostly self-explanatory, and were plotted against radius because (in the author's opinion) it is the most intuitive way to look at a spherical body, and additionally, plots versus radius contain the same information as plots versus mass, with the axes shifted. Notable in these plots is a check on the condition of hydrostatic equilibrium and a 'bump' in the individual compositions near the convective zone. The opacity was calculated using Kramer's law, a classical approximation to the solar opacity, and it experiences a minimum near the convective zone. Once an opacity was obtained, the logical next step was to look at the changing optical depth inside the star. Finally, one notices the strongly peaked distribution of ^{3}helium, in the solar interior. This is due to the fact that ^{3}helium is quickly consumed by the *pp* chains in the inner regions of the Sun, but has no mechanism for formation in the outer regions. In the peak region, ^{3}helium is produced via the first two reactions of *pp*-I, but temperatures are not high enough for the subsequent reaction to take place. Appendix B contains the *IDL* code used to produce all figures in this paper.

A. Additional figures

Figures created from standard solar model data.

A. IDL code used to produce figures

filename:/home/france/idl/solarmodel.pro

REFERENCES

J. Bahcall and R. Ulrich. Solar neutrinos and helioseismology. *Rev. Mod. Phys.*, 60:297+, April 1988.

Ahmad et al. Measurment of the rate of $\nu_e + \mathrm{d} \rightarrow \mathrm{p} + \mathrm{p} + e^-$ interactions produced by b solar neutrinos at the sudbury neutrino observatory. *Physical Review Letters*, 87:1+, August 2001.

W. Haxton. The solar neutrino problem. *Annu. Rev. Astron. Astrophys.*, 33:459–503, 1995.

R. Kippenhahn and A. Weigert. *Stellar Structure and Evolution.* Springer-Verlag, 1990.

S. Turck-Cheize, S. Cahen, M. Casse, and C. Doom. Revisiting the standard solar model. *The Astrophysical Journal*, 355:415–424, 1988.

M. Zeilik and S. Gregory. *Introductory Astronomy and Astrophysics.* Saunders, 1998.

This preprint was prepared with the AAS LATEX macros v5.0.

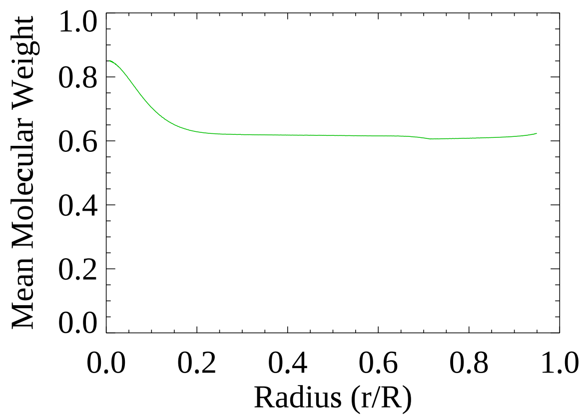

Fig. 1.— The mean molecular weight decreases in the outer regions of the star.

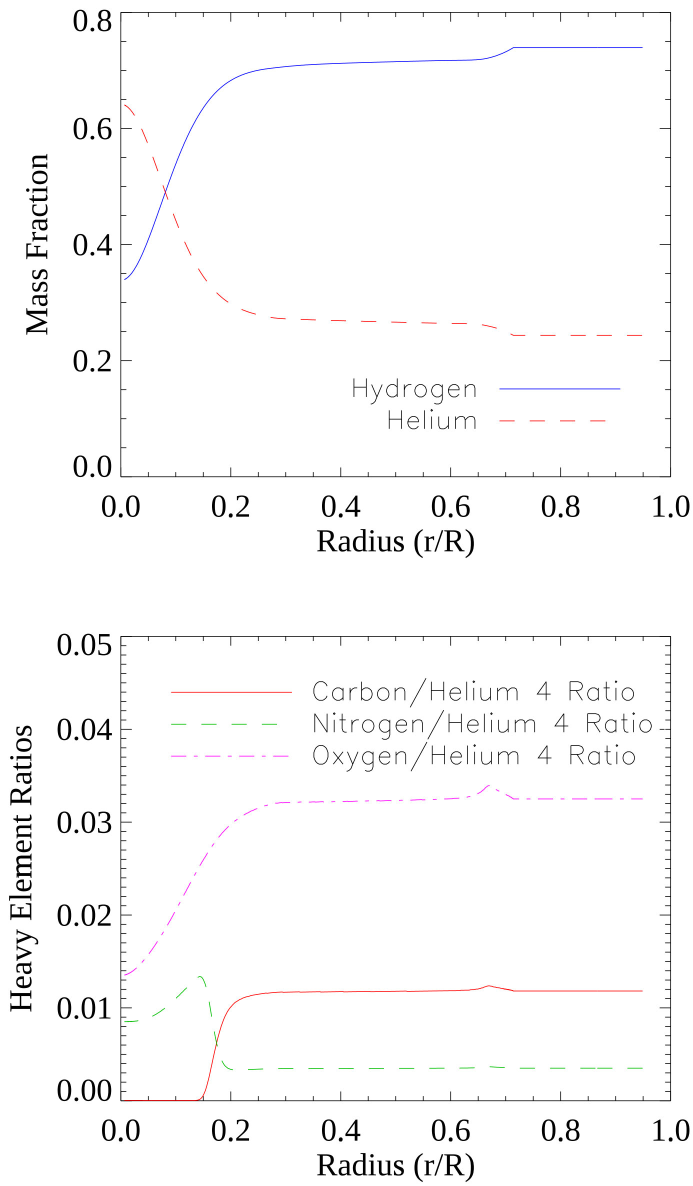

Fig. 2.— Enhanced helium and nitrogen abundances are evidence for stellar evolution.

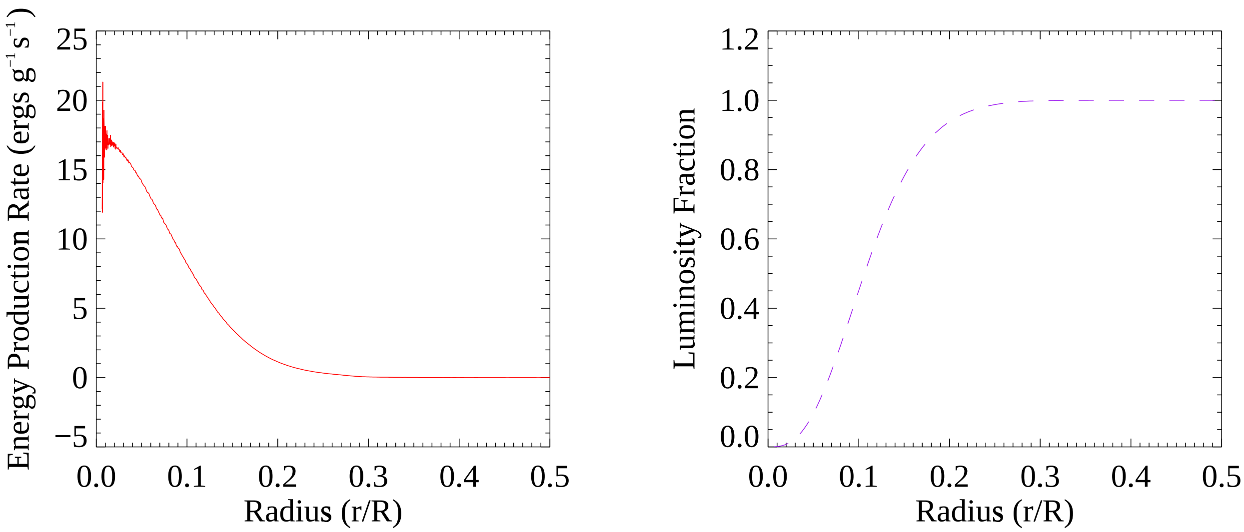

Fig. 3.— Most stellar energy production occurs in the core.

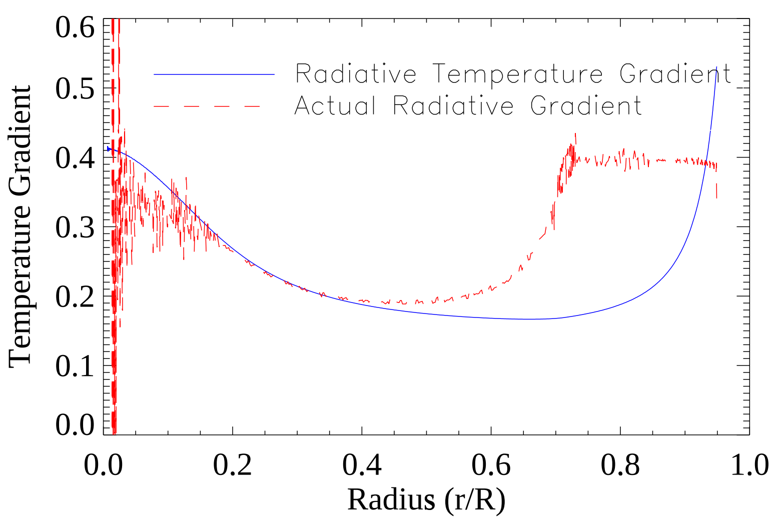

Fig. 4.— Convection becomes important when the star cannot transport all of its energy via radiation.

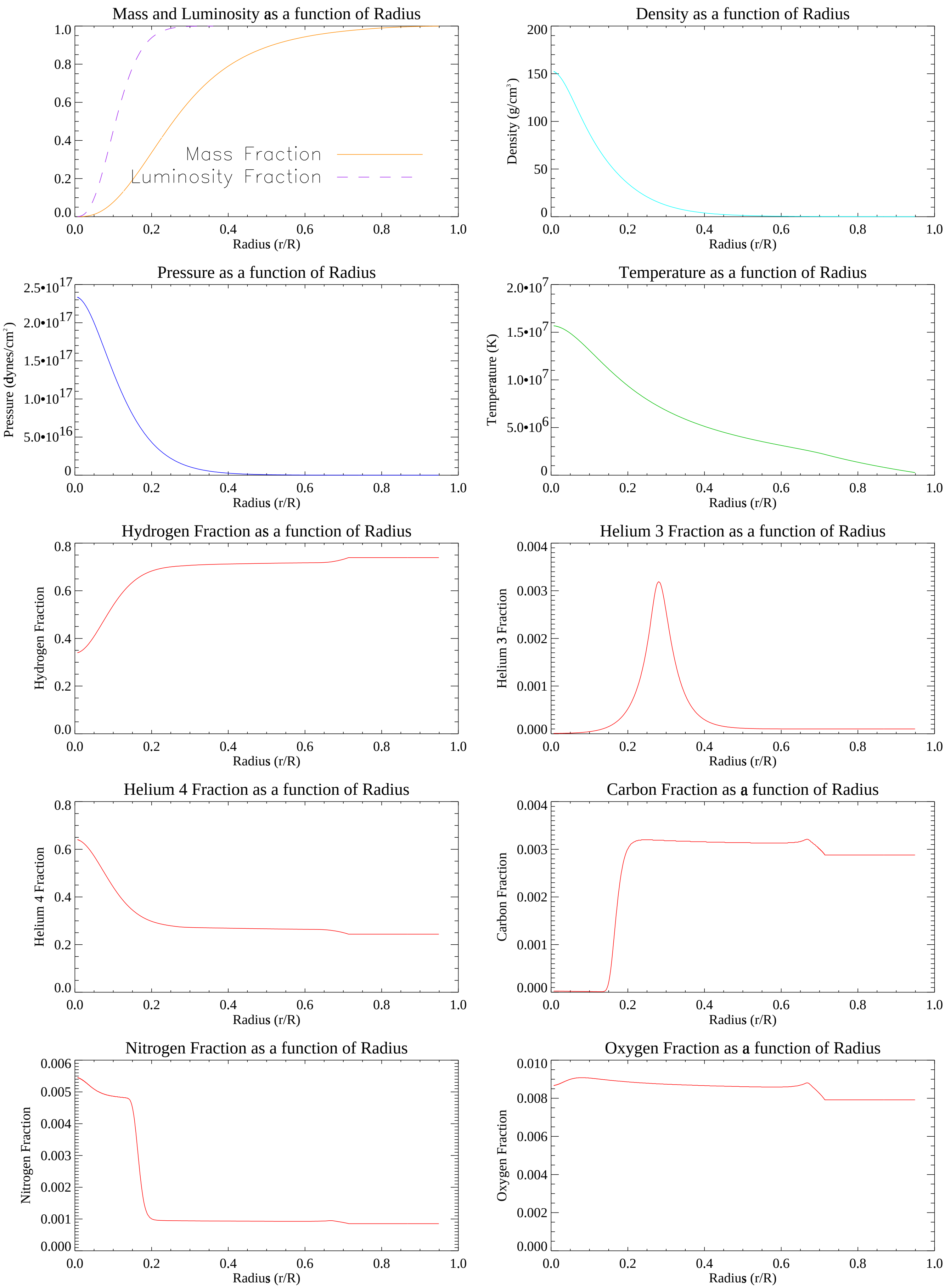
Mass and Luminosity as a function of Radius
Mass Fraction
Luminosity Fraction
Radius (r/R)
Density as a function of Radius
Density (g/cm³)
Radius (r/R)
Pressure as a function of Radius
Pressure (dynes/cm²)
Radius (r/R)
Temperature as a function of Radius
Temperature (K)
Radius (r/R)
Hydrogen Fraction as a function of Radius
Hydrogen Fraction
Radius (r/R)
Helium 3 Fraction as a function of Radius
Helium 3 Fraction
Radius (r/R)
Helium 4 Fraction as a function of Radius
Helium 4 Fraction
Radius (r/R)
Carbon Fraction as a function of Radius
Carbon Fraction
Radius (r/R)
Nitrogen Fraction as a function of Radius
Nitrogen Fraction
Radius (r/R)
Oxygen Fraction as a function of Radius
Oxygen Fraction
Radius (r/R)

Fig. 5.—

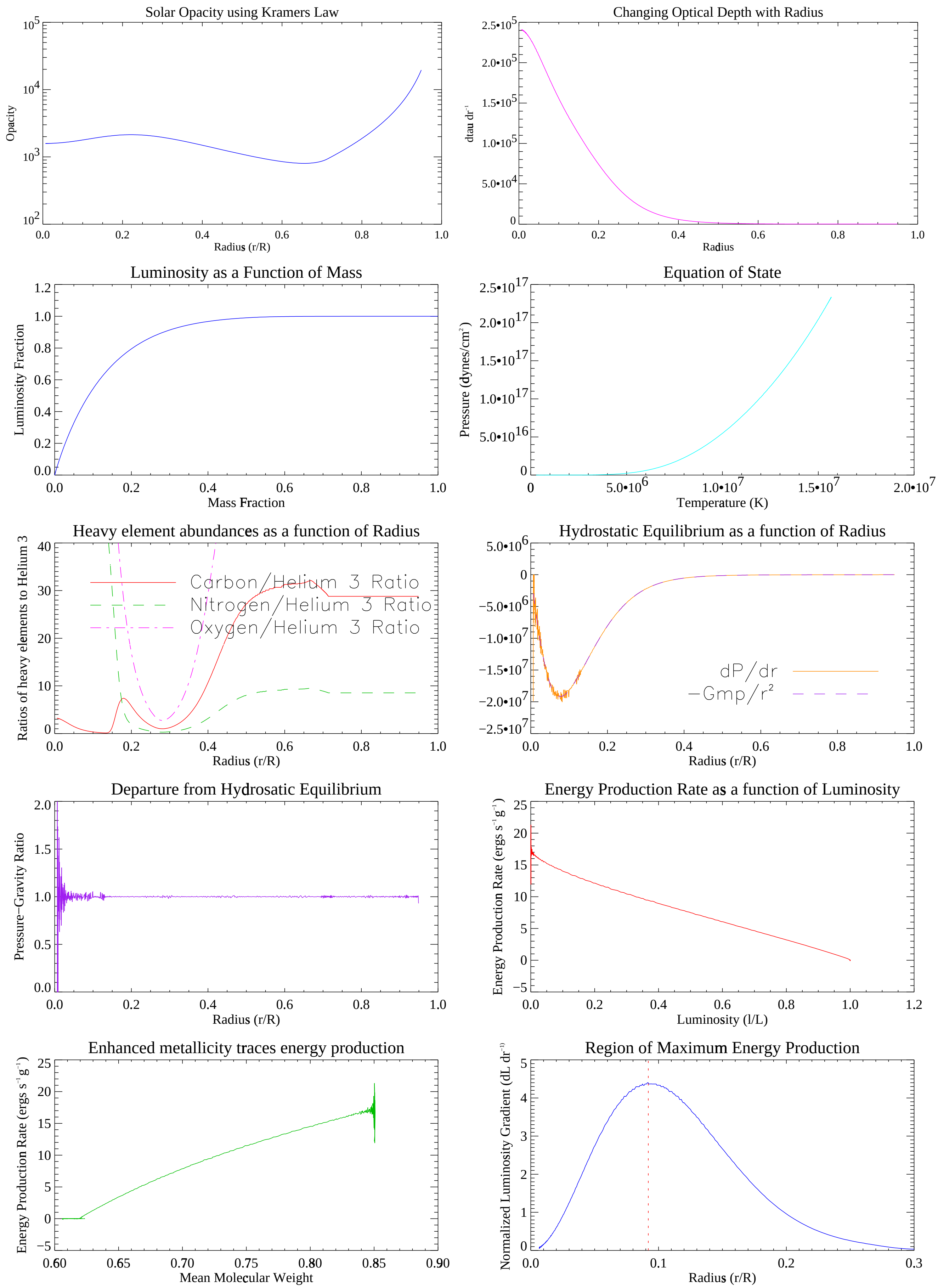

Solar Opacity using Kramers Law
Opacity
Radius (r/R)
Changing Optical Depth with Radius
dtau dr⁻¹
Radius
Luminosity as a Function of Mass
Luminosity Fraction
Mass Fraction
Equation of State
Pressure (dynes/cm²)
Temperature (K)
Heavy element abundances as a function of Radius
Ratios of heavy elements to Helium 3
Carbon/Helium 3 Ratio
Nitrogen/Helium 3 Ratio
Oxygen/Helium 3 Ratio
Radius (r/R)
Hydrostatic Equilibrium as a function of Radius
dP/dr
−Gmp/r²
Radius (r/R)
Departure from Hydrosatic Equilibrium
Pressure−Gravity Ratio
Radius (r/R)
Energy Production Rate as a function of Luminosity
Energy Production Rate (ergs s⁻¹ g⁻¹)
Luminosity (l/L)
Enhanced metallicity traces energy production
Energy Production Rate (ergs s⁻¹ g⁻¹)
Mean Molecular Weight
Region of Maximum Energy Production
Normalized Luminosity Gradient (dL dr⁻¹)
Radius (r/R)

Fig. 6.—